Supplementary Information

Construction of 3D flower like NiO/Mn_3O_4 heterojunction using Tulsi leaf extract for enhanced photodegradation of thiamethoxam pesticide and organic dyes under direct sunlight

Mandvi[a], Prit Pal Singh[a], Suhas Ballal[b], Mamta Chahar[c], Jaya Bansal[d], Ranvijay Kumar[e], Sandeep Kumar[f], Sandeep Kaushal[g]

[a] Sri Guru Granth Sahib World University, Fatehgarh Sahib, Punjab, India

[b]Jain (Deemed to be University), Banglore, Karnataka, India

[c]NIMS Institute of Engineering and Technology, NIMS University, Jaipur, Rajasthan, India

[d]Chandigarh Engineering College, Jhanjeri, Mohali, Punjab, India

[e] University Centre for Research and Development, Chandigarh University, Gharuan, Mohali, Punjab, India

[f]Akal University, Talwandi Sabo, Punjab, India

[g] Regional Institute of Education, NCERT, Ajmer, Rajasthan, India

Technique and instrumentation used for studies:

FTIR spectra of the nanocomposite were recorded using Perkin Elmer RXI FTIR spectrometer. The morphological investigations of the nanocomposite were done using FESEM (Carl Zeiss Supra 55) and HRTEM (Jeol Jem 2100 Plus). The structural nature of the heterojunction was studied by X-ray diffractometer (XRD, X'Pert PRO) at 2Θ = 10-70°. XPS (Thermo Fisher Scientific Escalab Xi^+) was employed to estimate the elemental composition of the metal oxides heterojunction. The adsorption parameters of metal oxides heterojunction were investigated by the Brunauer-Emmett-Teller (BET) method. Zeta-potential analysis was achieved using Zetasizer Nano-ZS90 (Malvern Inc.).

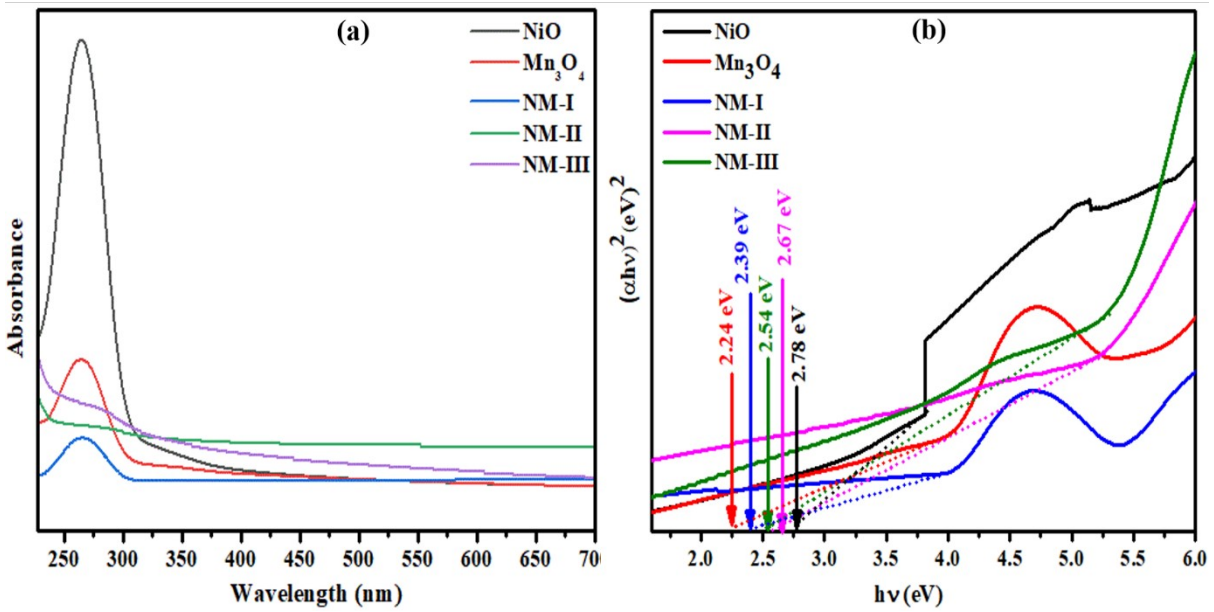

Fig. S1 a) XRD patterns of pure NiO, Mn_3O_4 and NiO/Mn_3O_4 heterojunction samples

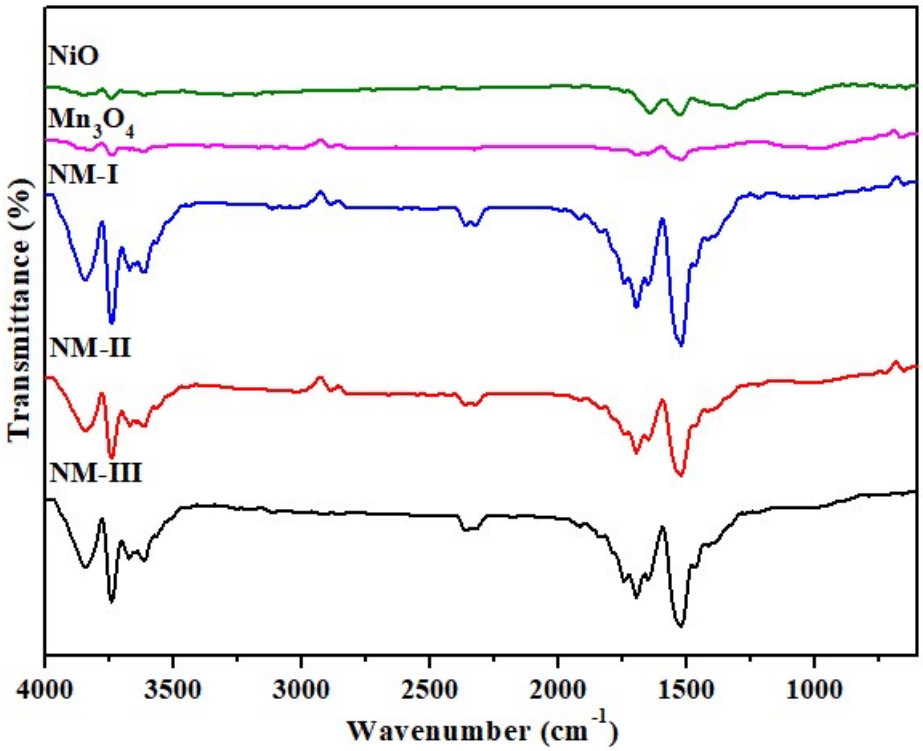

Fig. 2S. FTIR spectra of pure NiO, Mn_3O_4 and NiO/Mn_3O_4 heterojunction samples

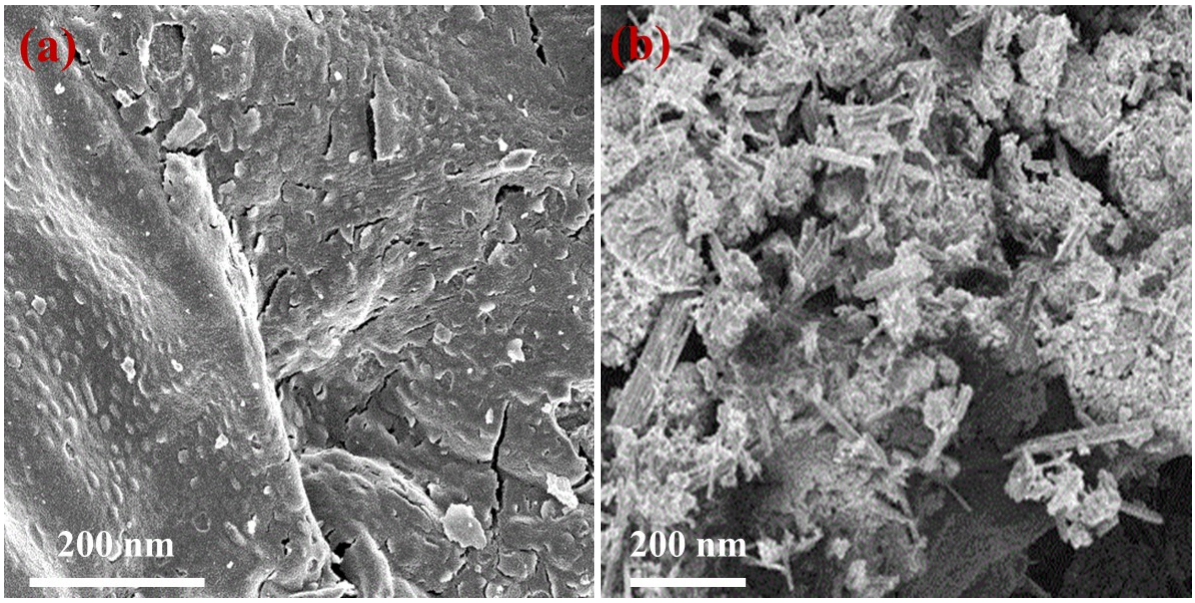

Fig. 3S Field-emission scanning electron microscopy images of a) NiO nanoparticles and b) Mn_3O_4 nanoparticles

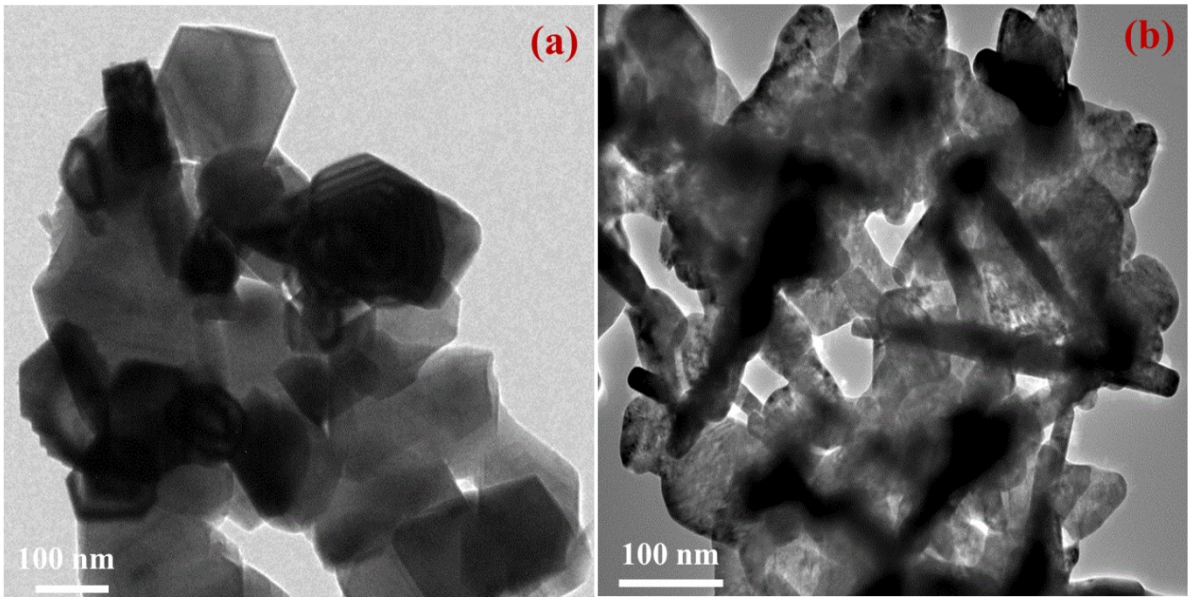

Fig. 4S High resolution transmission electron microscopy images of a) NiO nanoparticles and b) Mn_3O_4 nanoparticles

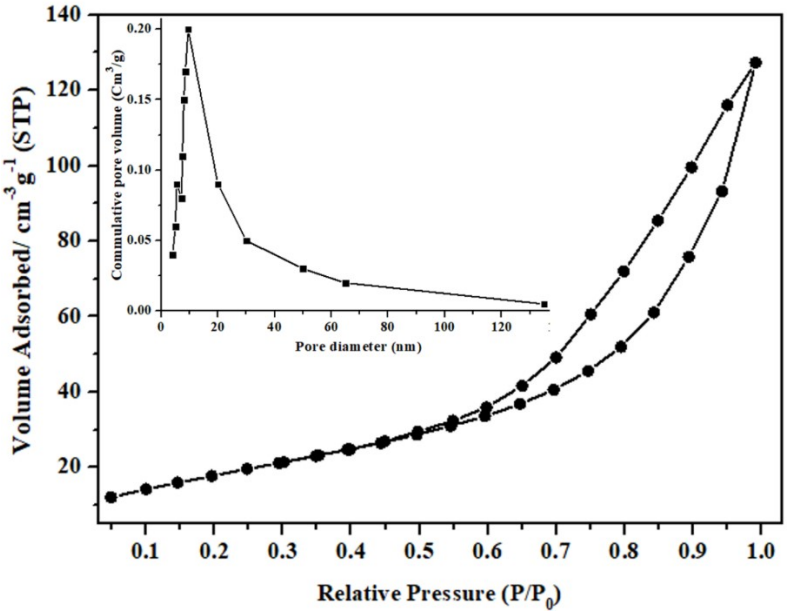

Fig. S3. N2 adsorption–desorption isotherm curves of NiO/Mn_3O_4 of heterojunction (inset: pore size distributions)

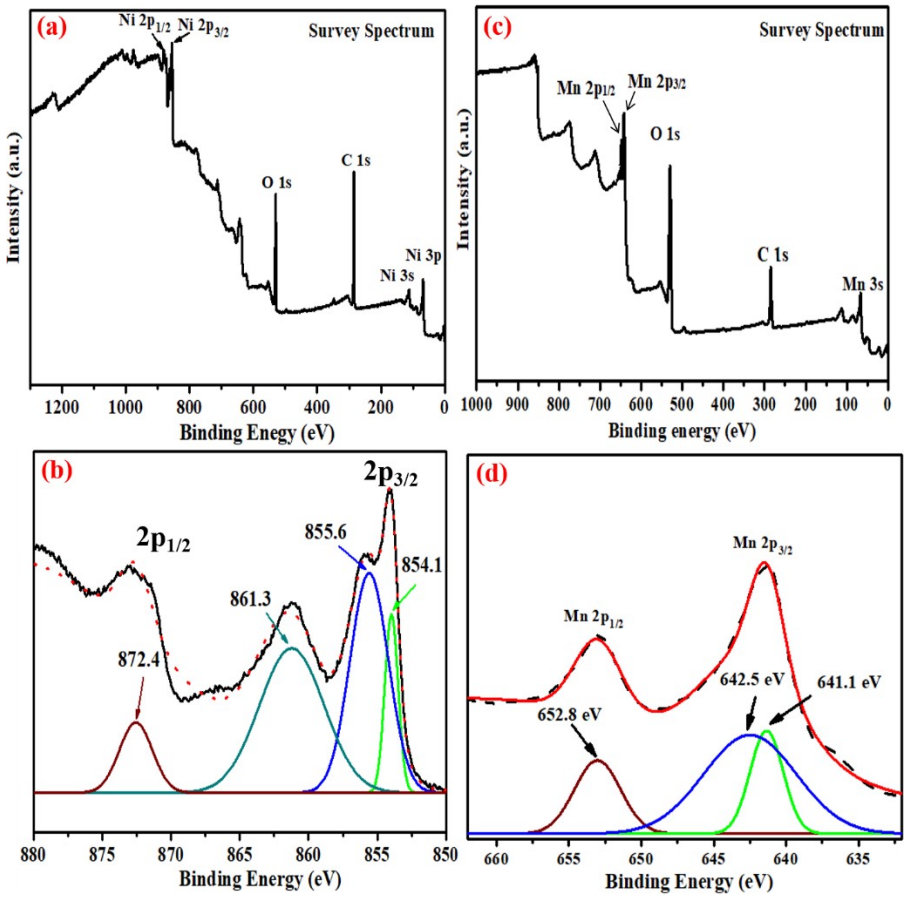

Fig. S6 High resolution XPS spectra of a, b) NiO and c, d) Mn_3O_4 NPs

The distinctive binding energy (eV) peaks related to Ni, O, and C in the NPs are evident in the survey spectrum (Fig. S5a). Ni $2p_{3/2}$ and Ni $2p_{1/2}$ peaks are supported by the observed Ni 2p spectra. The typical peaks of Ni^{2+} $2p_{3/2}$ and its satellite peaks have been identified at 854.1, 855.6, and 861.3 eV, each, as shown in Fig. S5b. In contrast, the Ni^{2+} $2p_{1/2}$ peak was detected at 872.6 eV, suggesting the formation of NiO structures. Similarly, the survey spectrum of Mn_3O_4 NPs revealed the presence of Mn, O and C elements in the metal oxide NPs (Fig. 5c). The 2p peak generates two potential states, $2p_{3/2}$ and $2p_{1/2}$, as a result of spin-orbit splitting of Mn (Fig. S5d). Of these, the Mn^{2+} state is associated with two peaks at 641.1 eV (Mn 2p3/2) and 652.8 eV (Mn 2p1/2), whereas the Mn^{4+} state is linked to the remaining peak at 642.5 eV (Mn $2p_{3/2}$).

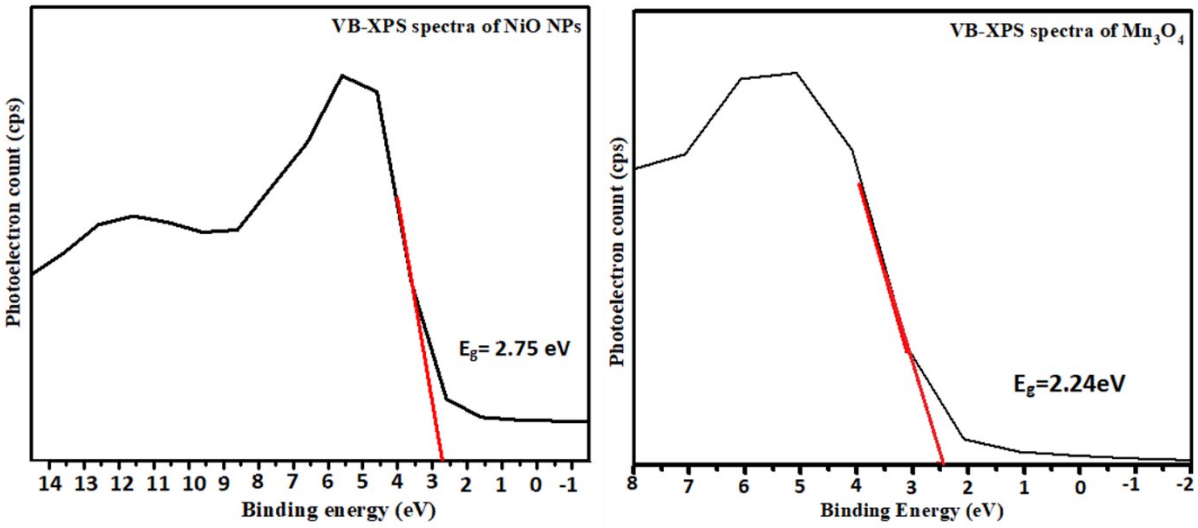

Fig. S7. VB-XPS spectra of NiO and Mn_3O_4 nanoparticles.

Further, XPS was employed for the analysis of valence band maximum (VBM) values for NiO and Mn_3O_4 NPs. From VB-XPS, valence band energy corresponding to NiO was found to be 2.75 eV and for Mn_3O_4, valence band maxima was observed to be 2.24 eV as shown in Fig. S3. From these VBM values, conduction band (CB) energy was calculated by following the equation:

$$E_{CB} = E_{VB} - E_g$$

E_g value of NiO and Mn_3O_4 corresponds to 2.78 eV and 2.24 eV, respectively. Using the above equation, E_{CB} values obtained for NiO and Mn_3O_4 were – 0.13eV and – 0.05eV which proved to be outstanding for photocatalytic reaction.

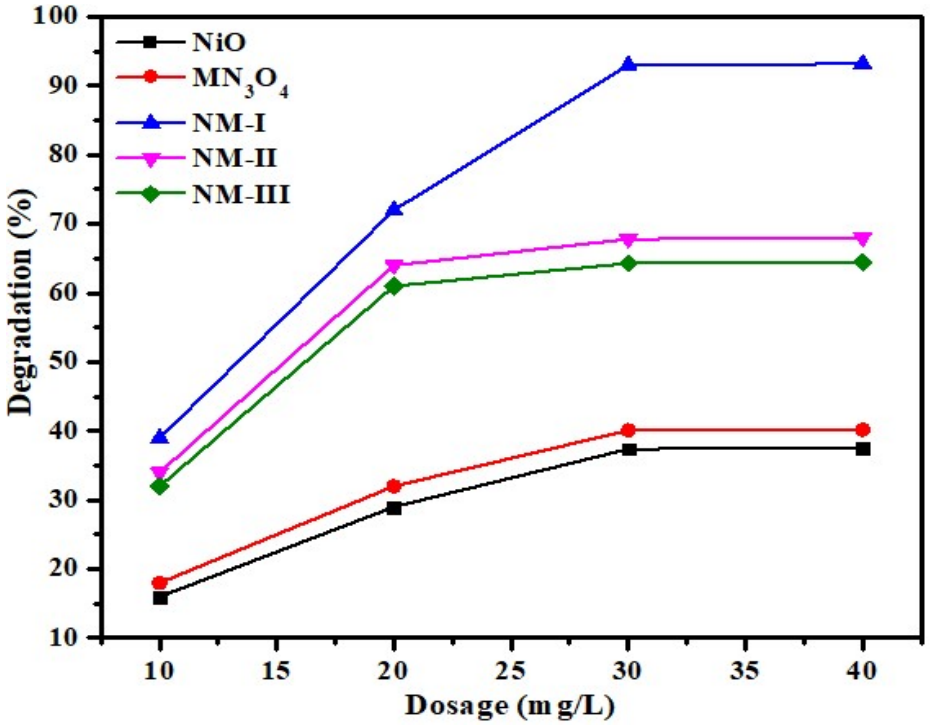

Fig. S8 Effect of dosage on percentage adsorption of THX

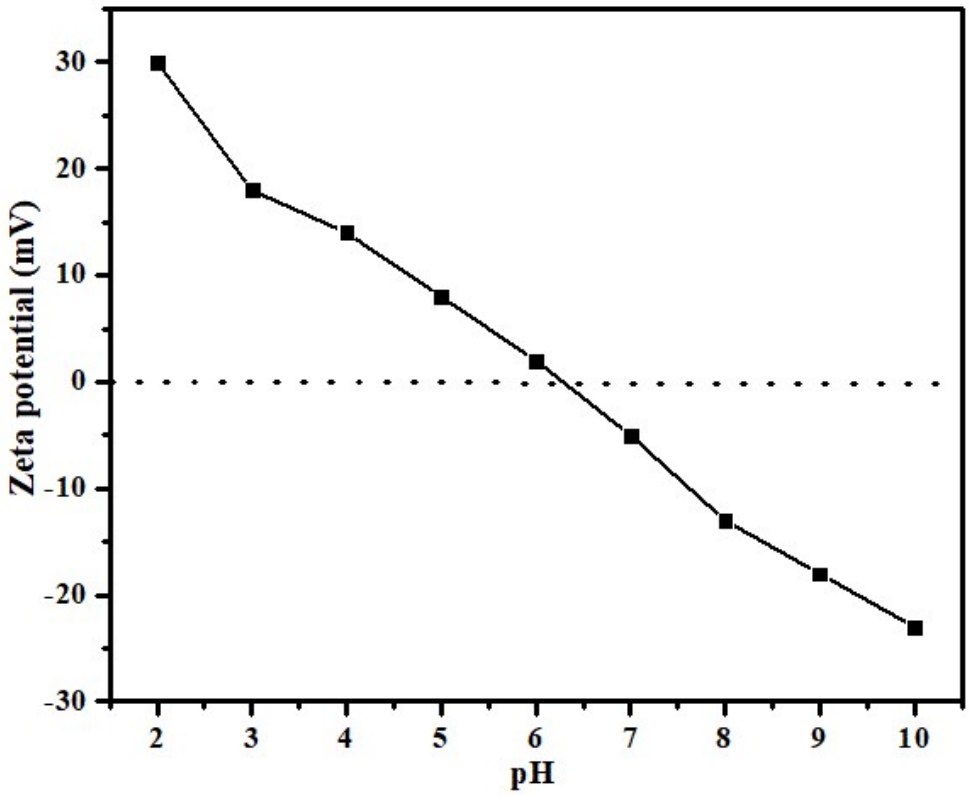

Fig. S9 Zeta potential of as synthesized NiO/Mn_3O_4 of heterojunction

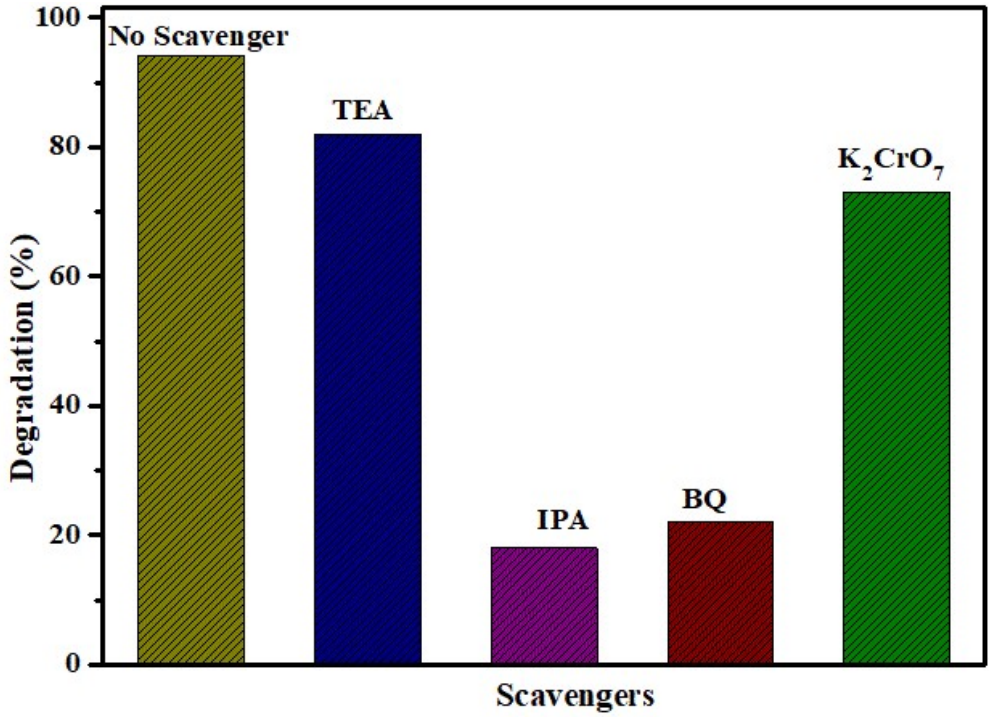

Fig. S10 Effect of scavengers on the degradation of TMX

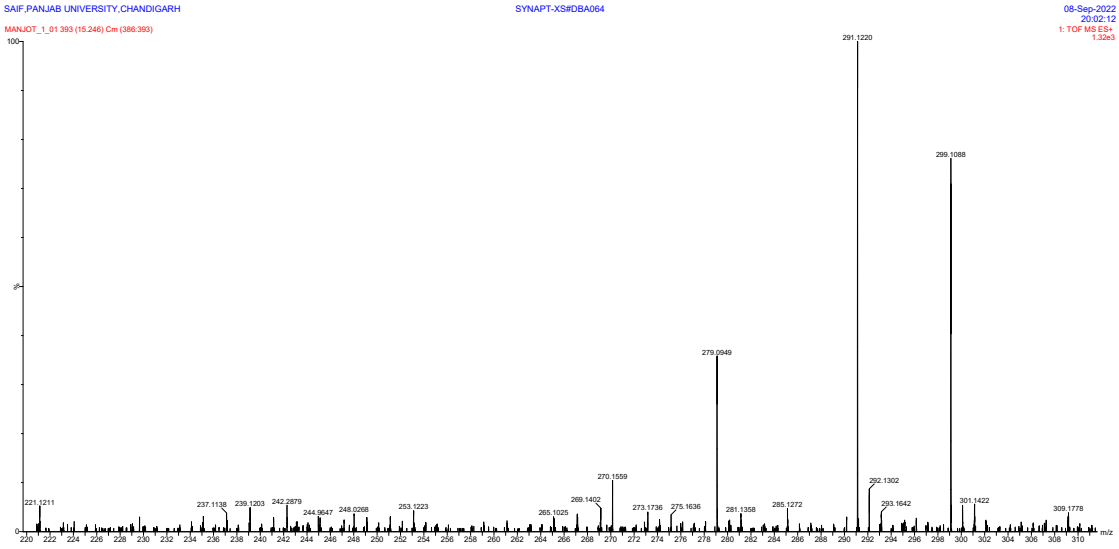

SAIF,PANJAB UNIVERSITY,CHANDIGARH

SYNAPT-XS#DBA064

08-Sep-2022
20:02:12

MANJOT_1_01 302 (11.714) Cm (301:305)

1: TOF MS ES+
277

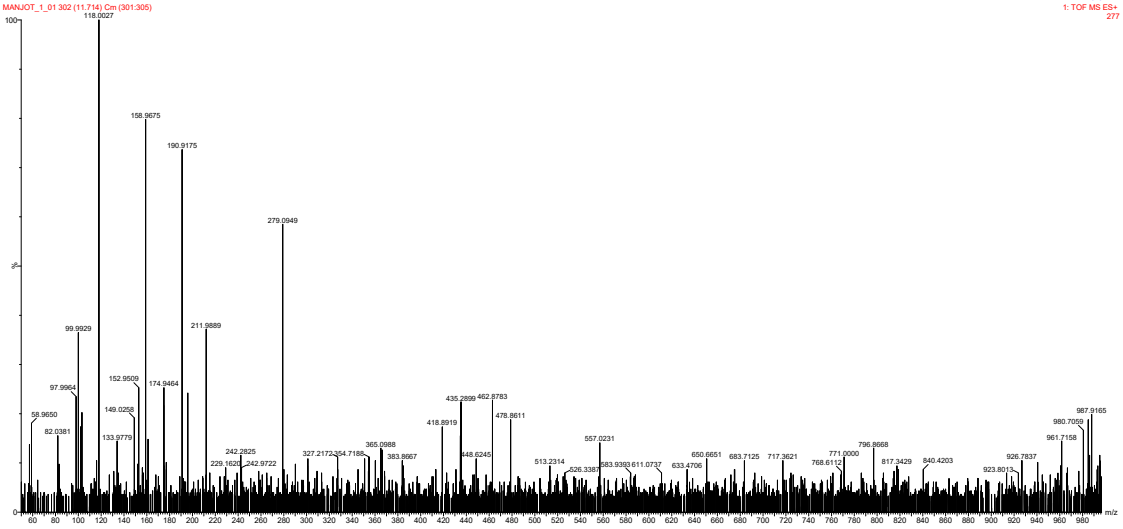

SAIF,PANJAB UNIVERSITY,CHANDIGARH

SYNAPT-XS#DBA064

08-Sep-2022
20:02:12

MANJOT_1_01 324 (12.556) Cm (322:328)

1: TOF MS ES+
2.77e6

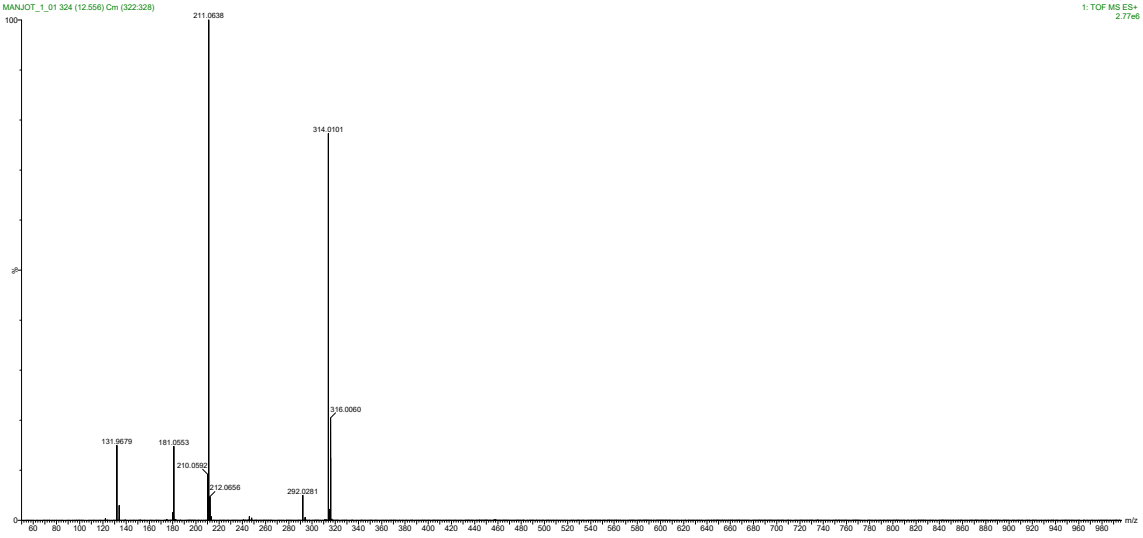

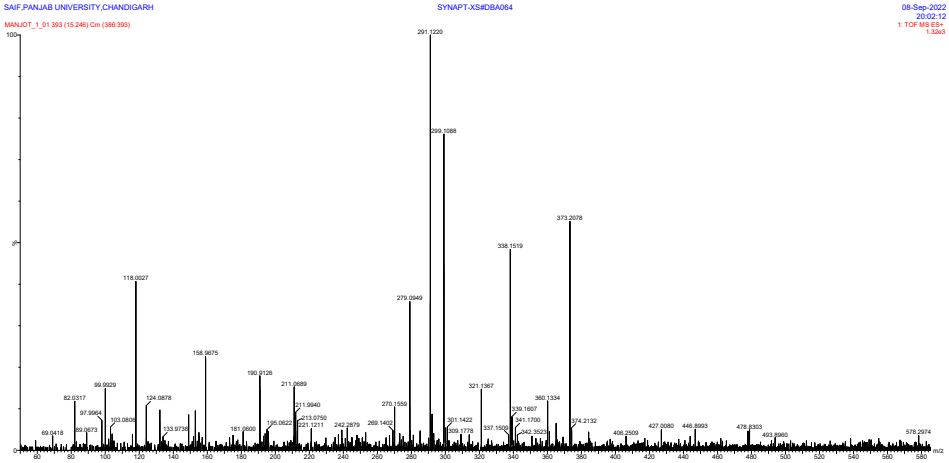
SAIF,PANJAB UNIVERSITY,CHANDIGARH
SYNAPT-XS#DBA064
08-Sep-2022
20:02:12
MANJOT_1_01 393 (15.246) Cm (386:393)
1: TOF MS ES+
1.32e3
291.1220
299.1088
373.3078
338.1519
118.0027
279.0949
158.9675
190.0126
211.0889
321.1367
99.9929
82.0317
124.0878
211.9940
213.0750
221.1211
97.9964
103.0806
133.9738
181.0600
195.0622
242.2679
269.1402
270.1559
301.1422
339.1607
341.1700
360.1334
374.2132
406.2509
427.0080
446.8993
478.8303
493.8960
578.2974
69.0418
99.0073
m/z

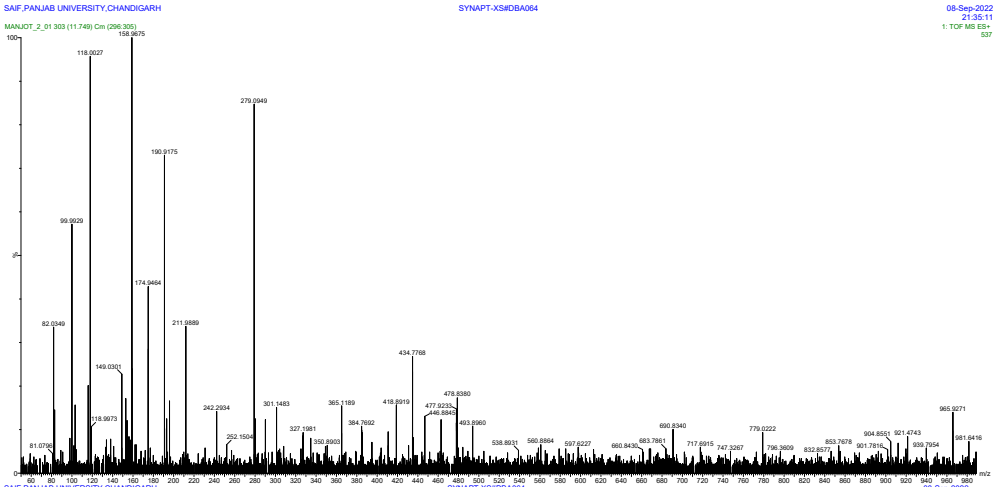
SAIF,PANJAB UNIVERSITY,CHANDIGARH
SYNAPT-XS#DBA064
08-Sep-2022
21:35:11
MANJOT_2_01 303 (11.749) Cm (296:305)
1: TOF MS ES+
537
158.9675
118.0027
279.0949
190.0175
99.9929
174.9464
82.0349
211.9889
434.7768
149.0301
478.8380
242.2934
301.1483
365.1189
418.3919
477.9233
446.8845
463.8960
384.7892
327.1981
150.8993
538.8931
560.8864
597.6227
660.8430
683.7861
690.8340
717.5915
747.3267
779.0222
796.3809
832.8577
853.7678
901.7815
904.8551
921.4743
939.7954
965.9271
981.8416
81.0706
252.1504
118.9973
m/z

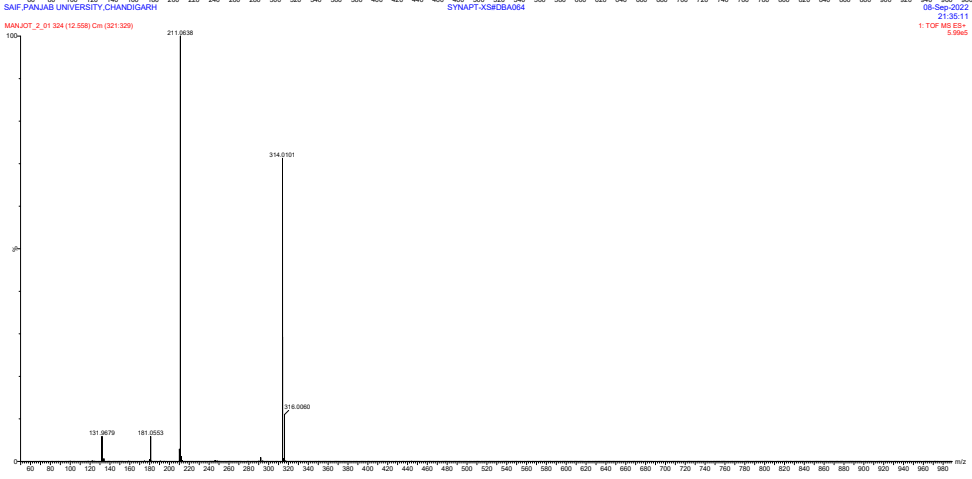
SAIF,PANJAB UNIVERSITY,CHANDIGARH
SYNAPT-XS#DBA064
08-Sep-2022
21:35:11
MANJOT_2_01 324 (12.558) Cm (321:329)
1: TOF MS ES+
5.99e5
211.0638
314.0101
316.0060
131.9679
181.0553
m/z

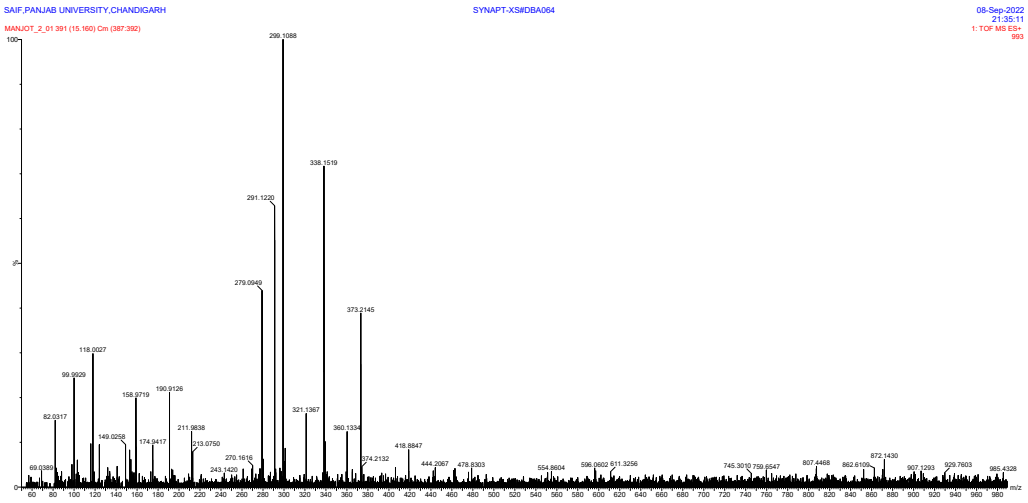

Fig. S11: LCMS-MS results obtained from photocatalytic degradation of THX insecticide.

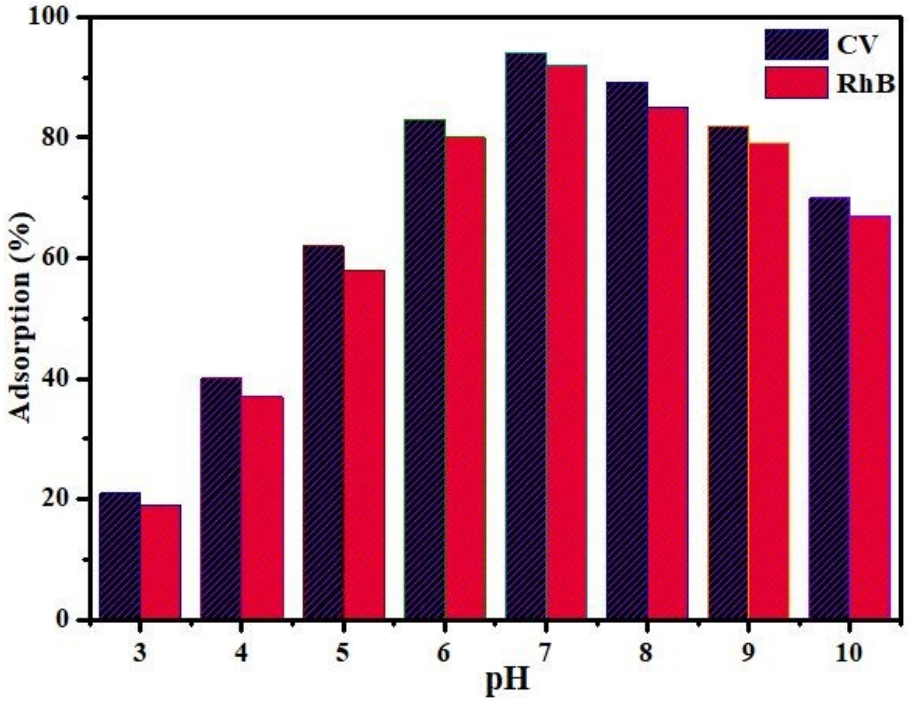

Fig S12. Effect of pH on the degradation of CV and RhB dyes

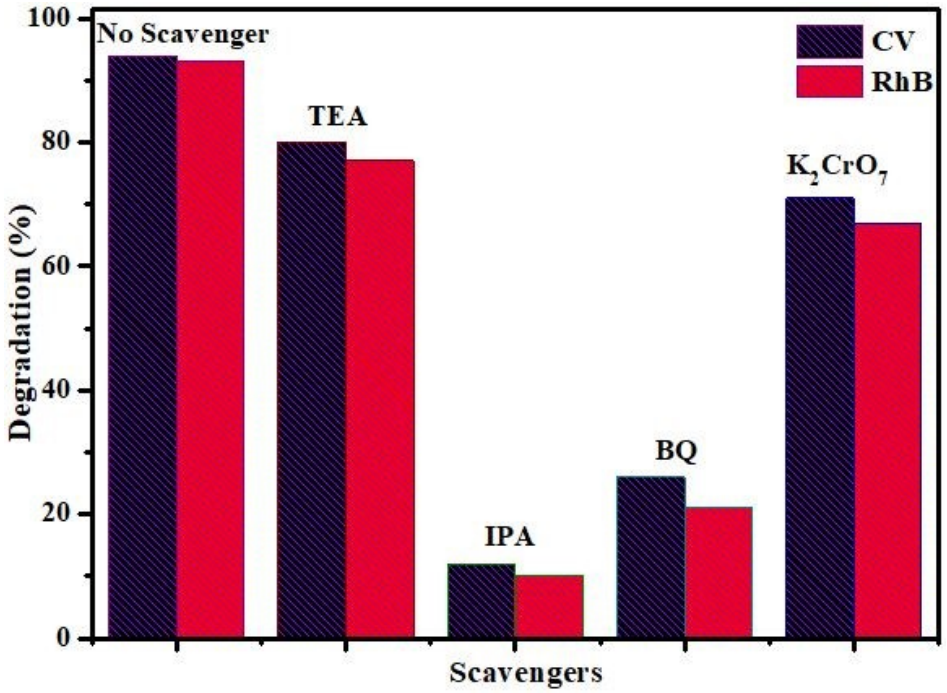

Fig S13. Effect of scavengers on the degradation of organic dyes

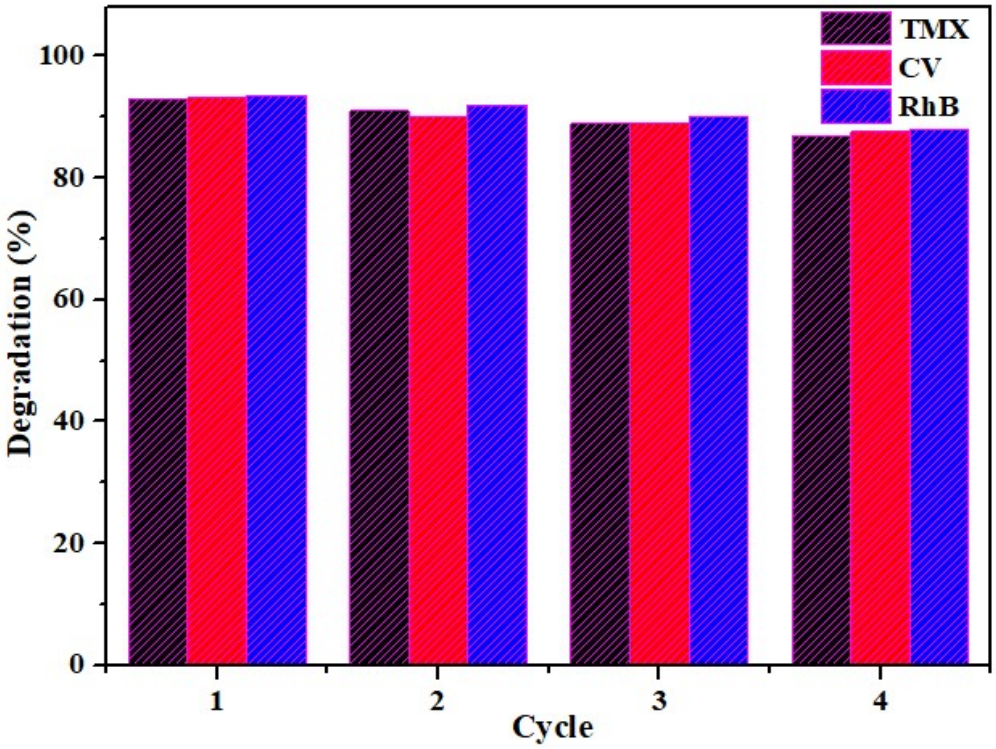

Fig. S14 Degradation efficiency of the NiO/Mn_3O_4 heterojunction (NM-I) for TMX, CV and RhB over four successive runs

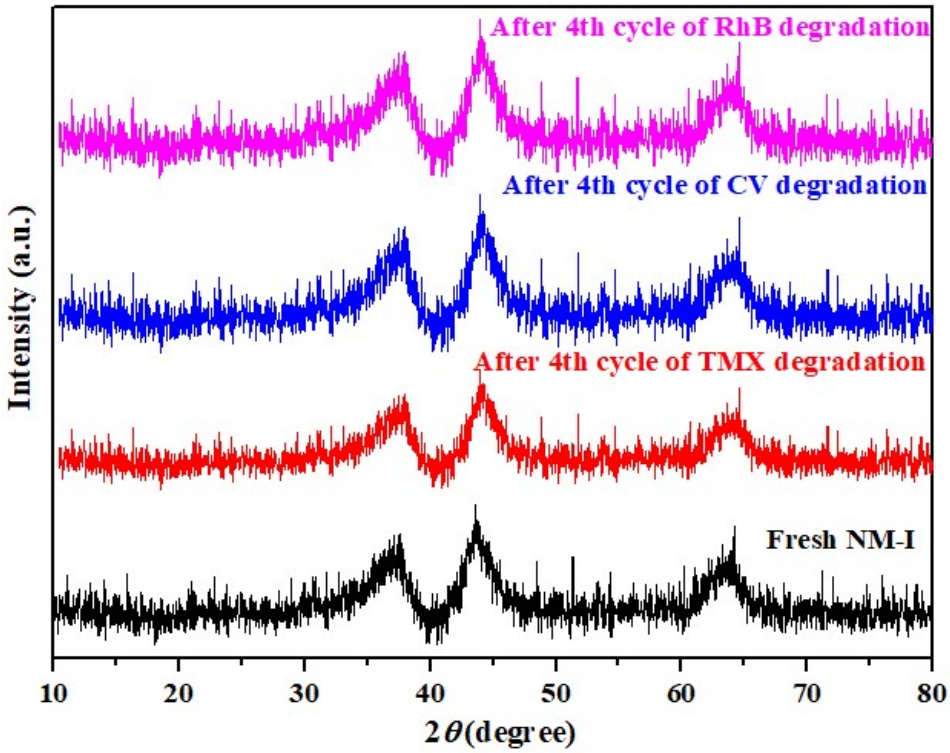

Fig. S15 XRD spectrum of NM-I photocatalyst before and after 4 successive photocatalysis cycles

Table

Table S1. The calculated values of various parameters for NiO/Mn_3O_4 heterojunction

Parameter	**NiO**	**Mn_3O_4**
E_g	3.2 eV	2.2 eV
E_{CB}	-0.35 eV	-0.03 eV
E_{VB}	+2.85 eV	2.17 eV